

Rapid and Versatile Construction of Diverse and Functional Nanostructures Derived from a Polyphosphoester-Based Biomimetic Block Copolymer System

Shiyi Zhang,^{†,‡} Jiong Zou,[†] Fuwu Zhang,[†] Mahmoud Elsabahy,^{†,§} Simcha E. Felder,[†] Jiahua Zhu,^{||} Darrin J. Pochan,^{||} and Karen L. Wooley^{*,†}

[†]Department of Chemistry, Department of Chemical Engineering, Laboratory for Synthetic-Biologic Interactions, Texas A&M University, P.O. Box 30012, 3255 TAMU, College Station, Texas 77842, United States

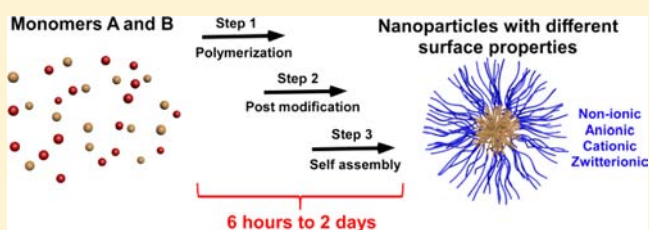
[‡]Department of Chemistry, Washington University in St. Louis, St. Louis, Missouri 63130, United States

[§]Department of Pharmaceutics, Faculty of Pharmacy, Assiut University, Assiut, Egypt

^{||}Department of Materials Science and Engineering, University of Delaware, Newark, Delaware 19716, United States

S Supporting Information

ABSTRACT: A rapid and efficient approach for the preparation and modification of a versatile class of functional polymer nanoparticles has been developed, for which the entire engineering process from small molecules to polymers to nanoparticles bypasses typical slow and inefficient procedures and rather employs a series of steps that capture fully the “click” chemistry concepts that have greatly facilitated the preparation of complex polymer materials over the past decade. The construction of various nanoparticles with functional complexity from a versatile platform is a challenging aim to provide materials for fundamental studies and also optimization toward a diverse range of applications. In this paper, we demonstrate the rapid and facile preparation of a family of nanoparticles with different surface charges and functionalities based on a biodegradable polyphosphoester block copolymer system. From a retrosynthetic point of view, the nonionic, anionic, cationic, and zwitterionic micelles with hydrodynamic diameters between 13 and 21 nm and great size uniformity were quickly formed by suspending, independently, four amphiphilic diblock polyphosphoesters into water, which were functionalized from the same parental hydrophobic-functional AB diblock polyphosphoester by click-type thiol–yne reactions. The well-defined (PDI < 1.2) hydrophobic-functional AB diblock polyphosphoester was synthesized by an ultrafast (<5 min) organocatalyzed ring-opening polymerization in a two-step, one-pot manner with the quantitative conversions of two kinds of cyclic phospholane monomers. The whole programmable process starting from small molecules to nanoparticles could be completed within 6 h, as the most rapid approach for the anionic and nonionic nanoparticles, although the cationic and zwitterionic nanoparticles required ca. 2 days due to purification by dialysis. The micelles showed high biocompatibility, with even the cationic micelles exhibiting a 6-fold lower cytotoxicity toward RAW 264.7 mouse macrophage cells, as compared to the commercial transfection agent Lipofectamine.



INTRODUCTION

Engineered nanoparticles with unique physical and chemical properties at the nanoscale, emulating natural nanosystems (e.g., viruses, lipoproteins, and proteins) in both structural and functional features, have been bringing about a revolutionary impact on the pharmaceutical industry, due to their applications as diagnostic, therapeutic, and theranostic agents for a wide variety of human diseases.^{1–5} Polymeric micelles exhibit similarities with natural nanobiosystems in their overall structural features and their programmed construction from small compounds (monomers) to macromolecules to functional nanoscopic self-assemblies. Micellar nanostructures have attracted great attention for their distinctive core–shell morphology and their tunable sizes and chemistries in both the core and shell regions by using different functionalized

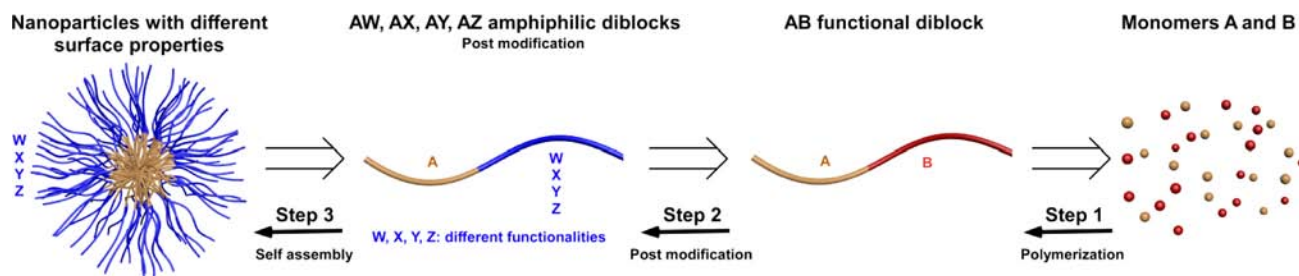
block copolymers.⁶ Recent advances in polymerization methodologies and the application of reactive, efficient, and orthogonal functionalization reactions, such as “click” chemistries, have enabled the engineering of functional block polymers to direct their self-assembly into nanoparticles with various sizes, surface charges, and functionalities.^{7–12} However, it is still challenging to rapidly construct a biodegradable system that serves as a versatile platform, beginning from the point of small molecules and engineering them stagewise toward multifunctional nanoparticles with tunable properties.

The standard retrosynthetic analysis of Scheme 1 allows for the preparation of a series of polymeric nanoassemblies having

Received: September 11, 2012

Published: October 23, 2012

Scheme 1. Retrosynthetic Analysis of Polymeric Micelles with Different Surface Properties



different coronal compositions and properties, by the assembly of a family of diblock copolymers with different functionalities along one of the block segments defined from postpolymerization modifications of a single diblock copolymer type that is prepared from the polymerization of functional monomers. The key challenge with this approach is to achieve rapid and efficient chemical and physical transformations at each of the three steps. By taking advantage of modern polymerization methodologies, a variety of nondegradable and degradable amphiphilic block copolymers have been synthesized, with the incorporation of orthogonal chemistries and possessing capability for supramolecular assembly in water (step 1). Click chemistry has provided a library of chemical reactions for the chemical transformations of the specific functionalities installed in the initial polymerization step and have greatly expedited step 2.¹³ However, the advantageous features of click chemistry in step 2, such as quantitative conversion, rapid reaction, mild conditions, high functional group tolerance, and an absence of byproducts and side reactions, have not been fully realized by the overall series of steps, due to the polymerizations in step 1 and the self-assembly processes in step 3 usually being time-consuming, or involving incomplete conversion of monomers, or harsh reaction conditions.⁹ Herein, we demonstrate a novel strategy to program a series of diverse, functional nanostructures from reactive monomers, in which all three steps are rapid, quantitative, and conducted under mild conditions.

Our programmable platform toward various nanoparticles is based on polyphosphoesters. Like polyesters, polypeptides, and polycarbonates, polyphosphoesters are attractive for biomedical applications, such as gene delivery, imaging, drug delivery, and tissue engineering, due to their biocompatibility, biodegradability, and structural similarity to nucleic and teichoic acids.^{14–16} As a result of the intrinsic degradability, the functionalization of polyesters, polypeptides, and polycarbonates has additional challenges over nondegradable systems. Beyond those typical degradable polymers, however, the functionalities and properties of polyphosphoesters are conveniently controlled by manipulation of pendant groups on the pentavalent phosphorus atom of cyclic phospholane monomer precursors. Since the retrosynthetic analysis reverts ultimately to the monomers, we designed and synthesized two kinds of cyclic phospholane monomers: one that carried an alkyne functionality for polymerization into segment B, followed by conversion into functional hydrophilic block segments (W, X, Y, Z), and the other is a hydrophobic monomer that led to the common segment A. As polyphosphoesters are a relatively new type of synthetic polymer, the hydrophobic cyclic phospholane monomer 2-ethylbutyl phospholane was developed to overcome the hydrophilic nature of the polyphosphoester backbone. The polymerization

activity of this novel monomer upon two organocatalysts was studied and compared with that of our recently reported functional monomer, butynyl phospholane.¹⁷ In step 1, organocatalyzed ring-opening polymerizations (ROP) were employed to fully convert the two monomers sequentially into the well-defined (PDI < 1.2) hydrophobic functional AB diblock polyphosphoester in an ultrafast (<5 min) one-pot manner by utilizing the reactivity difference between the two monomers. Click-type thiol–yne reactions, in step 2, were applied to functionalize this parental hydrophobic functional diblock precursor into four amphiphilic diblock copolymers with different charge types, such as nonionic, anionic, cationic, and zwitterionic. In the final step, a series of uniform polymeric micelles with different surface charges and functionalities was quickly achieved by directly dissolving each polymer material into water. Detailed physicochemical and biological studies of the polymeric micelles with different surface properties were conducted to understand the effect of surface functionalities on their behaviors. This programmable process greatly facilitates the preparation of degradable functional nanoparticles, when all advantageous features of click-type chemical concepts were realized in each step of this strategy.

RESULTS AND DISCUSSION

Rapid and facile construction of diverse nanostructures is demonstrated starting from the simple syntheses of functional cyclic phospholane monomers and continuing at each stage through polymerization, chemical modification, and supramolecular assembly steps. Ultrafast (<5 min) one-pot sequential polymerization of two different cyclic phospholane monomers produced a single hydrophobic-functional AB diblock polyphosphoester, having reactive alkynyl side-chain chemical functionalities within only the B block segment. After its rapid (<1 h) purification by precipitation and centrifugation, a series of thiol–yne chemical transformations produced four different functionalized diblock copolymers that were then assembled by direct dissolution into water to afford four different polymeric micelles with tunable surface properties.

Monomer Design and Synthesis. Polyphosphoesters can be prepared by ring-opening polymerization (ROP),¹⁸ polycondensation,¹⁹ transesterification,²⁰ and enzymatic polymerization.²¹ Among all of these methods, the ROP of cyclic phospholane monomers by using metal compounds as initiators or polymerization catalysts is a well-established process to provide linear or hyperbranched polyphosphoesters²² with predictable molecular weight, narrow molecular weight distribution, and well-defined chain ends.²³ Recently, Iwasaki et al. first reported using 1,8-diazabicyclo[5.4.0]undec-7-ene (DBU) or 1,5,7-triazabicyclo[4.4.0]dec-5-ene (TBD) as organocatalysts to promote ROP of cyclic phospholanes.²⁴ To eliminate using environmentally sensitive metal compounds,

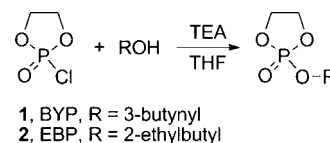
and better fulfill the requirements of biomedical applications, many groups have adopted the organocatalyzed ROP of phospholanes to prepare polyphosphoesters for biomaterials.^{17,22,25–28}

Two phospholane monomers were required for our design: one having a reactive chemical functionality that would be stable during polymerization and then readily available for chemical modification and the second providing hydrophobicity, ultimately to lead to amphiphilic block copolymers for assembly of nanostructures. Cyclic phospholane monomers are usually prepared from the condensation of 2-chloro-2-oxo-1,3,2-dioxaphospholane (COP) and an alcohol. A variety of functional cyclic phospholane monomers have been reported, including methyl,²⁹ ethyl,³⁰ isopropyl,³¹ PEG-ylated,^{32,33} hydroxyl-functionalized,^{34,35} protected hydroxyl-functionalized,³⁶ protected amino-functionalized,^{37,38} protected thiol-functionalized,³⁹ acrylate-functionalized,⁴⁰ methacrylate-functionalized,⁴¹ alkyne-functionalized,¹⁷ and alkene-functionalized.^{27,28} The ROP of those functional monomers produced corresponding high molecular weight functional polyphosphoesters. Our group recently developed a stable alkyne-functionalized cyclic phospholane monomer and studied its polymerization kinetics under an organocatalyst, in addition to the chemical functionalization of this alkyne-functionalized polyphosphoester by click-type azide–alkyne Huisgen cycloaddition and thiol–yne reaction.¹⁷ This butynyl phospholane (BYP, **1**) monomer was, therefore, used to incorporate side chain chemical functionality along the backbone of one segment of the AB block copolymer of this study, to allow for the versatile platform development.

A challenge associated with identification of the second phospholane monomer, for production of a hydrophobic polyphosphoester chain segment that could be utilized to drive supramolecular assembly into nanostructures in water, is related to the high water solubility of the polyphosphoester backbone. The hydrophobicity of the polyphosphoester system can be tuned by changing the alkyl side chains of the monomer or by copolymerizing monomers with different alkyl side chains, but the water solubility of alkyl-substituted polyphosphoesters has been typically observed to be temperature-dependent.^{29,30} For instance, a hydrophobic monomer, 2-isopropoxy-2-oxo-1,3,2-dioxaphospholane, produced an isopropyl-functionalized polyphosphoester that exhibited a lower critical solution temperature (LCST) and when incorporated into a diblock copolymer, poly(ethylene glycol)-*block*-poly(2-isopropoxy-2-oxo-1,3,2-dioxaphospholane), served as a hydrophobic domain of an amphiphilic core–shell morphological nanoparticle only at temperatures above its LCST.^{25,42} To achieve a polyphosphoester with high hydrophobicity over a wide temperature range, we attempted to couple COP with several alcohols with long or bulky alkyl groups. A tertiary alcohol, *tert*-butanol, was employed to react with COP, but the product monomer decomposed in the reaction mixture. The cyclic phospholane monomer from the coupling of a secondary alcohol, 3-pentanol, and COP also decomposed upon heating during vacuum distillation. The boiling point of 1-decanol and that of the resulting monomer were too similar to allow for good purification. To avoid the poor purification abilities, 2-ethyl-1-butanol was chosen to functionalize COP because of its relatively bulky hydrophobic alkyl group. Finally, the monomer, 2-ethylbutyl phospholane (EBP, **2**), was obtained through the one-step esterification of two commercially available com-

pounds, 2-ethyl-1-butanol and COP, followed by simple filtration and vacuum distillation (Scheme 2).

Scheme 2. Synthesis of Cyclic Phospholane Monomers from COP and Primary Alcohols



Homopolymerization of EBP by Organocatalysts. The polymerization behavior of **2** with organocatalysts DBU or TBD was studied (Table 1). The polymerizations of **2** upon addition of DBU (entries 1–3 in Table 1) were conducted at room temperature to allow the direct comparison to our published polymerization results of BYP.¹⁷ In our previous report, the conversion of **1** reached 99% in 10 min with different ratios of monomer-to-initiator. In contrast, the conversion of **2** did not reach 60% even over a period of 1 h under the same conditions, which suggested that the reactivity of **2** is much lower than that of **1**, potentially because of the sterically bulky side chain. Also, DBU gave poor control over the molecular weight distribution (PDI > 1.30) for the polymerization of **2**. When TBD was used as a catalyst instead of DBU, the polymerization of **2** proceeded to 99% conversion in less than 5 min at 0 °C (entries 4–6 in Table 1). The dual activation of TBD, simultaneously serving as a hydrogen-bond donor to the monomer via the N–H site and also as a hydrogen-bond acceptor to the hydroxyl proton of the propagating alcohol, explains the significant increase in the polymerization rate.²⁷ When the polymerization of **2** with TBD was quenched by acetic acid upon the completion of the reaction, good control over the molecular weight distribution (PDI < 1.20) could be achieved. Therefore, well-defined poly(2-ethylbutyl phospholane) (PEBP, **3**) with predictable molecular weight could be synthesized by using TBD as a catalyst.

One-Pot Sequential ROP. To prepare diblock polyphosphoester, we first attempted to polymerize **1** and then **2** by using TBD or DBU as a catalyst and benzyl alcohol as an initiator (Supporting Information, Scheme S1). After the complete conversion of the first monomer **1**, the second monomer **2** was added into the reaction mixture. However, there was no conversion of **2** (monitored by ³¹P NMR) and no chain extension (characterized by DMF GPC). We speculated that TBD or DBU associated predominately with poly(butyryl phospholane) (PBYP) or residual **1** over **2**, due to the bulky side chain of **2**. Therefore, when **1**, PBYP, and catalyst (TBD or DBU) were all present in the reaction mixture neither catalyst was able to successfully promote the ROP of **2** to achieve chain extension.

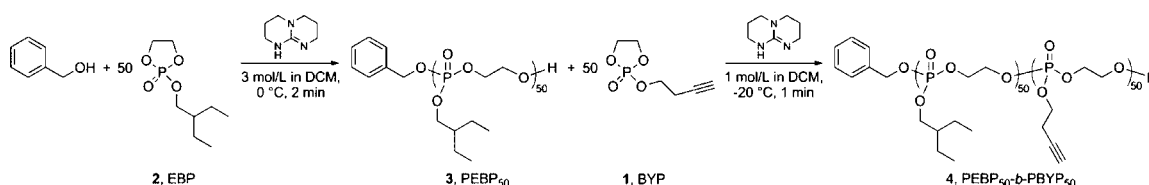
Successful chain extension was achieved and poly(2-ethylbutyl phospholane)₅₀-*b*-poly(butyryl phospholane)₅₀ (PEBP₅₀-*b*-PBYP₅₀, **4**) was synthesized after the addition order of the two monomers in the sequential polymerization was reversed (Scheme 3). The less reactive monomer, **2**, was first polymerized at relatively high concentration in dichloromethane with TBD as a catalyst and benzyl alcohol as an initiator at 0 °C. After complete conversion of **2** (monitored by ³¹P NMR) in 2 min, the more reactive monomer, **1**, was transferred into the reaction mixture for the chain extension.

Table 1. Polymerization Results of **2** with DBU and TBD under Different Conditions

entry	catalyst	M:I:catalyst (molar ratios) ^a	temp	time (min)	% conversion (³¹ P NMR)	M _n , Da			M _w /M _n ^b
						GPC ^b	Theor ^c	¹ H NMR ^d	
1	DBU	25:1:1.5	rt	15	51	5600	2700	3000	1.31
2	DBU	50:1:1.5	rt	30	43	6700	5600	5200	1.34
3	DBU	100:1:1.5	rt	60	32	8300	6800	7100	1.42
4	TBD	25:1:1.5	0 °C	1	99	7100	5300	5600	1.14
5	TBD	50:1:1.5	0 °C	2	100	10300	10400	11000	1.14
6	TBD	100:1:1.5	0 °C	4	99	17200	21000	20500	1.16

^aConcentrations for all entries were 1 g of monomer (M) per 1 mL of dichloromethane. Initiator (I) was benzyl alcohol for all entries. ^bM_n and M_w/M_n were measured by DMF GPC calibrated using polystyrene standards. ^cM_n was calculated from the monomer to initiator ratio and corrected for conversion. ^dM_n was calculated from the monomer to initiator ratio based on ¹H NMR of final polymer product.

Scheme 3. Synthesis of PEBP₅₀-*b*-PBYP₅₀, **4**, Diblock Polyphosphoester Bearing a Hydrophobic Block (PEBP) and a Functional Block (PBYP) via a One-Pot Sequential ROP



Over 99% conversion of **1** was reached quickly (in 1 min); however, GPC analysis of the diblock polymer showed poor control over the molecular weight distribution and the possibility of transesterification (Supporting Information, Figure S1). To decrease the polymerization rate as well as the possibility of transesterification, the second step of sequential polymerizations was conducted at lower monomer concentration and $-20\text{ }^{\circ}\text{C}$ by diluting and cooling the reaction mixture before the second monomer was added. A 2 min polymerization of **2** at $0\text{ }^{\circ}\text{C}$ and 3 mol/L monomer concentration and the sequential 1 min polymerization of **1** at $-20\text{ }^{\circ}\text{C}$ and 1 mol/L monomer concentration provided over 99% conversion of each monomer in the individual steps and retained a narrow molecular weight distribution with a PDI of 1.17 for the diblock polyphosphoester (Figure 1). The diblock

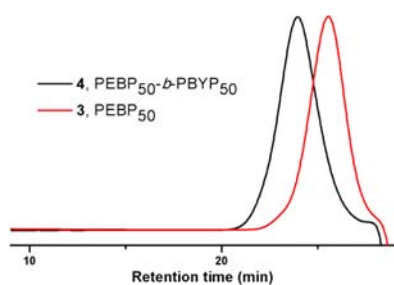


Figure 1. GPC traces of PEBP₅₀ at M_n = 9800 g/mol and PDI = 1.14 (red line) and PEBP₅₀-*b*-PBYP₅₀ diblock copolymer at M_n = 16 700 g/mol and PDI = 1.17 (black line) produced by the one-pot sequential ROP.

copolymer **4** was easily purified by precipitation from dichloromethane or acetone into a pentane and diethyl ether mixture (3:1 vol ratio) followed by centrifugation.

This facile polymerization provided a strategy to prepare diblock polyphosphoester with precise structural control in an atom-efficient synthesis manner.⁴³ Confirmation of the diblock composition was made by ³¹P NMR spectroscopy of the purified polymer, which displayed two signals at -1.19 and

-1.83 ppm that were assigned to the two ³¹P environments in the PEBP and PBYP blocks, respectively (Figure 2). ¹H NMR

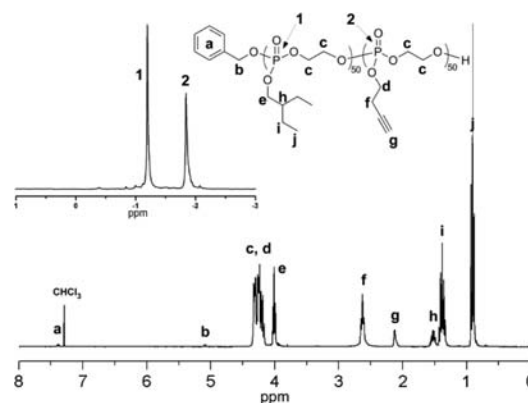


Figure 2. ¹H NMR and ³¹P NMR (upper left inset) spectra (CDCl₃) of purified PEBP₅₀-*b*-PBYP₅₀ diblock copolymer.

also showed full retention of the alkyne group of the functional PBYP block and alkyl group in hydrophobic PEBP block. The sequential polymerization of two monomers in a one-pot method at multigram scale was completed in less than 5 min, and the three precipitations and centrifugations could be accomplished in less than 1 h. The ultrafast one-pot sequential synthesis of a well-defined diblock polyphosphoester is more advantageous than the chain extension from purified macro-initiator, which requires the complete removal of acetic acid used for quenching the first polymerization step.²⁷

Functionalization by Thiol–Yne Reactions. The hydrophobic-functional AB diblock polyphosphoester, **4**, was then functionalized into four amphiphilic diblock polyphosphoesters by click-type thiol–yne reaction with thiol-containing molecules including 2-(2'-methoxyethoxy)ethanethiol, 3-mercaptopropionic acid, cysteamine hydrochloride, and L-cysteine hydrochloride monohydrate (Scheme 4). Radical-mediated thiol–yne chemistry, a click-type reaction, is a robust and versatile method that tolerates a variety of functional groups,

Scheme 4. Schematic Representation of the Functionalizations of PEBP₅₀-*b*-PBYP₅₀ with Four Different Charged or Noncharged Thiols and the Self-Assembly of Four Resulting Amphiphilic Diblock Copolymers: Nonionic Block Copolymer (5), Anionic Block Copolymer (6), Cationic Block Copolymer (7), and Zwitterionic Block Copolymer (8) into Four Micelles, 9–12, Respectively, with Different Surface Charges

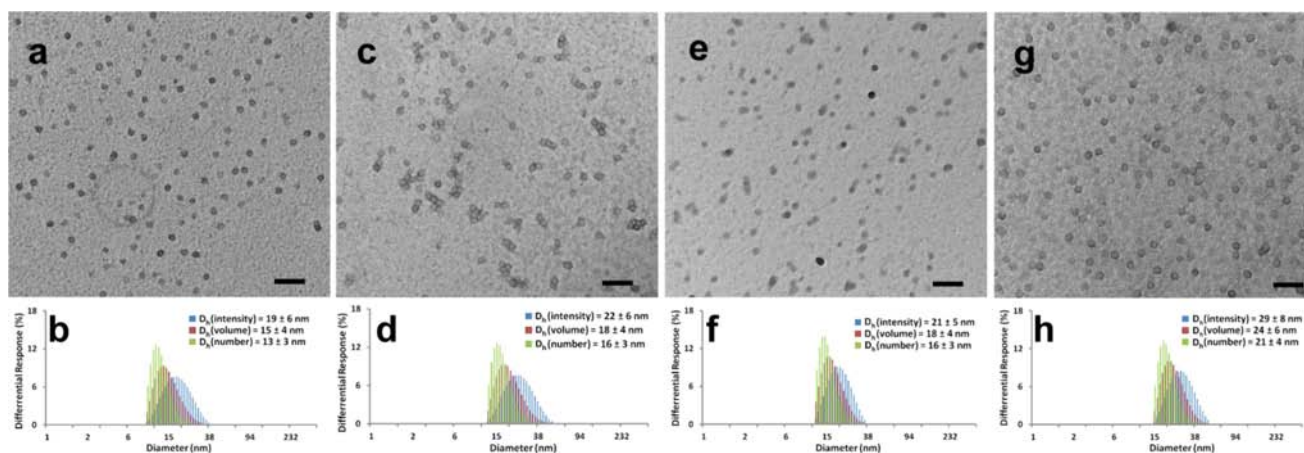
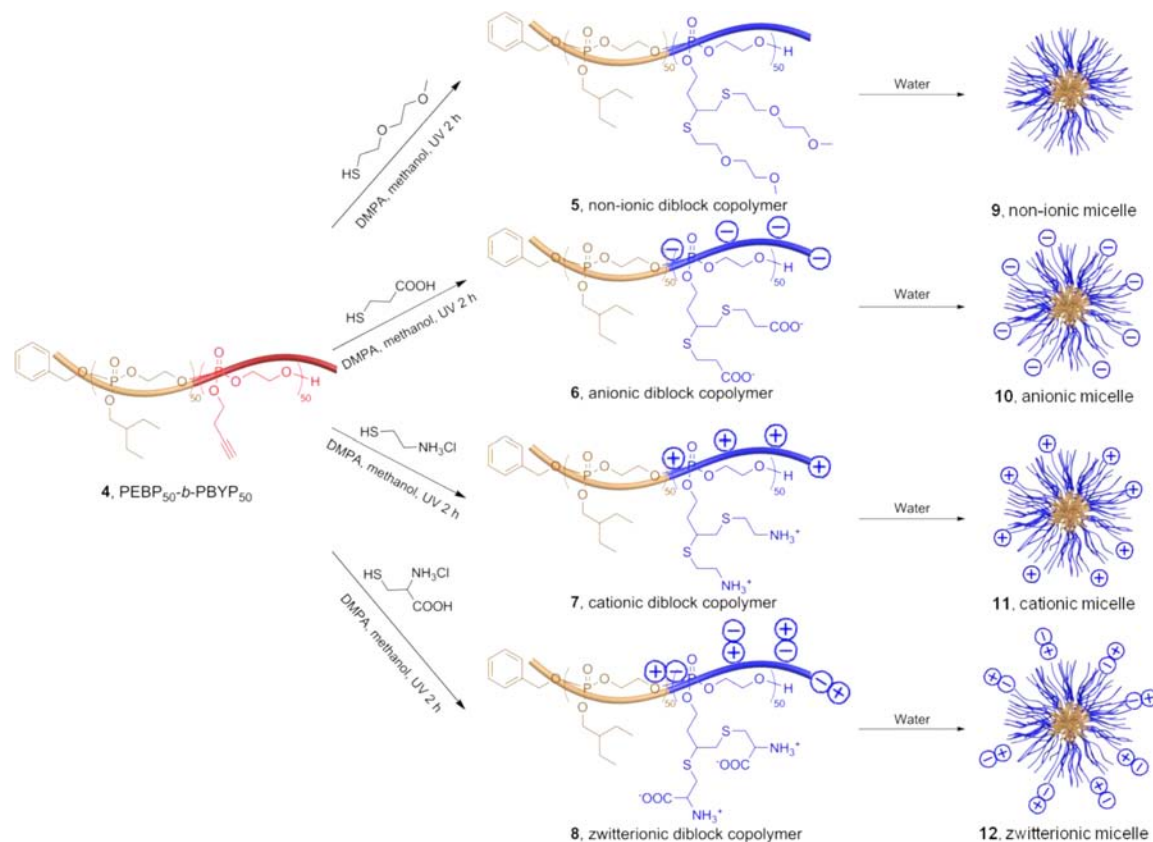


Figure 3. Self-assembly results of nonionic micelle **9** (a, e), anionic micelle **10** (b, f), cationic micelle **11** (c, g), and zwitterionic micelle **12** (d, h) in nanopure water. (a) TEM image of **9**, the average diameter of which is 15 ± 3 nm, after counting more than 100 particles. (b) DLS results of **9**: $D_h(\text{intensity}) = 19 \pm 6$ nm, $D_h(\text{volume}) = 15 \pm 4$ nm, $D_h(\text{number}) = 13 \pm 3$ nm. (c) TEM image of **10**, the average diameter of which is 18 ± 4 nm, after counting more than 100 particles. (d) DLS results of **10**: $D_h(\text{intensity}) = 22 \pm 6$ nm, $D_h(\text{volume}) = 18 \pm 4$ nm, $D_h(\text{number}) = 16 \pm 3$ nm. (e) TEM image of **11**, the average diameter of which is 18 ± 5 nm, after counting more than 100 particles. (f) DLS results of **11**: $D_h(\text{intensity}) = 21 \pm 5$ nm, $D_h(\text{volume}) = 18 \pm 4$ nm, $D_h(\text{number}) = 16 \pm 3$ nm. (g) TEM image of **12**, the average diameter of which is 23 ± 3 nm, after counting more than 100 particles. (h) DLS results of **12**: $D_h(\text{intensity}) = 29 \pm 8$ nm, $D_h(\text{volume}) = 24 \pm 6$ nm, $D_h(\text{number}) = 21 \pm 4$ nm. All scale bars in TEM images are 100 nm.

such as carboxylic acids and amines, to densely functionalize alkynyl groups.⁴⁴ In our previous report, we demonstrated that the radical-mediated thiol–yne reaction was compatible with the polyphosphoester backbone without causing any coupling

or cross-linking.¹⁷ Ten equivalents of thiols to alkynyl groups were used in the radical reaction to avoid chain–chain coupling, while 2 h exposure to UV irradiation with DMPA as the photoinitiator ensured complete conversion.

Each functionalized diblock copolymer was readily purified and its structure was confirmed. Given the use of 10-fold excess amounts of the thiols, the conditions employed for purification were defined by their physical characteristics. The nonionic diblock, **5**, and anionic diblock, **6**, could be purified by direct precipitation from methanol or acetone into a pentane and diethyl ether (3:1 vol ratio) three times and dried under vacuum. However, the salt-based thiols required that the cationic diblock, **7**, and zwitterionic diblock, **8**, were purified by dialysis against a pH 3.0 HCl solution, an acidic condition to ensure the amine group was protonated, in a cold room (4–8 °C) for 2 days and then lyophilized. The disappearance of the terminal acetylene protons (2.18–2.04 ppm) in the ^1H NMR spectra of the four product polymers confirmed the full consumption of the alkyne groups. The diastereotopic splitting of the methylene protons (1.76–1.92, 2.31–2.47 ppm), corresponding to the 1,2-regioselectivity of thiol–yne chemistry, and the presence of other functional groups also verified the successful installation of the four different thiols onto **4**. The thiol–yne reaction was demonstrated to efficiently transform the hydrophobic-functional AB diblock polyphosphoester into four different kinds of amphiphilic polyphosphoesters. Besides thiol–yne reactions, other reactions on the alkynes could be conducted; for instance, another click-type reaction, azide–alkyne Huisgen cycloaddition, is being employed to efficiently functionalize the hydrophobic-functional AB diblock polyphosphoester with poly(ethylene glycol) (PEG). The preparation and application of PEG-ylated polyphosphoester-based nanoparticles are currently underway in our group.

Self-Assembly of Amphiphilic Polyphosphoesters. All four amphiphilic polyphosphoesters were dissolved in nanopure water by sonication for 5 min at room temperature and spontaneously formed spherical nanoparticles, **9–12**, with narrow size distributions (Figure 3). The glass transition temperatures (T_g) were far below room temperature (–50 °C), so all polymer chain segments, whether hydrophilic or hydrophobic, had sufficient mobility and were able to undergo rapid relaxation or extension in response to the varied electrostatic interactions to self-organize into micellar structures with core–shell morphology easily. In the nanoparticle assemblies, it is expected that the hydrophobic PEBP block aggregated in the particle core and was shielded from the aqueous medium by the shell region consisting of functionalized PBYP blocks, due to the highly hydrophilic nature of the oligo(ethylene glycol), carboxyl, and amino groups.

The morphological influence of varying PBYP block functionalities on the aqueous self-assembled nanoparticles was characterized by both transmission electron microscopy (TEM) and dynamic light scattering (DLS). Bright-field TEM images of **9**, **10**, **11**, and **12** prepared in nanopure water showed uniform particles with average sizes of approximately 15, 18, 18, and 23 nm, respectively (Figure 3, parts a, b, c, and d, respectively). Due to the collapsing of swelled hydrophilic block chains during dry TEM sample preparation, the core–shell architecture was not directly observed. DLS results showed monomodal size distribution of particles in all four aqueous assembly samples. The number-average hydrodynamic diameter values ($D_h(\text{number})$) of **9**, **10**, **11**, and **12** were 13 ± 3 , 16 ± 3 , 16 ± 3 , and 21 ± 4 nm, respectively (Figure 3, parts e, f, g, h, respectively). Due to differences in the hydrophilic–hydrophobic balance and potential repulsive effects within and between hydrophilic chains with the same micellar assemblies,

those constructed from the anionic (**6**) or cationic (**7**) functionalized PBYP chains were of slightly increased particle sizes than the nonionic (**5**) functionalized PBYP chains, as measured by both TEM and DLS results. Zwitterionic functionalized polymer **8** assembled into particles with the largest particle size; however, all of the particle sizes were similar. It is remarkable that such uniform particle size distributions were produced by a simple, rapid, direct dissolution of the bulk block copolymer samples into nanopure water or buffer solutions.

Surface Charges of the Micelle Systems. The surface charge densities, measured as ζ -potential values, were characterized for the resulting micelles in pH 5.0 and 7.4 buffer solutions by a Delsa Nano C particle analyzer (Figure 4).

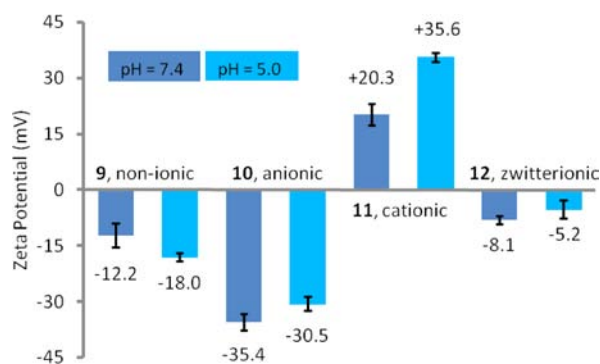


Figure 4. ζ -Potential values of **9–12** in PBS buffer solutions at pH 7.4 and pH 5.0. The average values and their standard deviations, from six measurements, are shown.

Nonionic micelles, **9**, were slightly negatively charged with ζ -potentials of –12.2 mV at pH 7.4 and –18.0 at pH 5.0, which is common for neutral polymer nanoparticles, including those based on polyphosphoesters.^{15,36} The anionic and cationic characteristics of micelles formed from **10** and **11** were confirmed through ζ -potential measurements. The anionic micelles were more negatively charged at pH 7.4 than at pH 5.0 due to the higher degree of deprotonation of carboxylic groups at pH 7.4 than at pH 5.0. Similarly, because of a higher extent of protonation of amino groups at pH 5.0 than at pH 7.4, the cationic micelles were more positively charged at pH 5.0 than at pH 7.4. In the case of the zwitterionic micelles, the positive charge of amino groups and the negative charge of carboxylic groups counteracted each other, which resulted in almost neutral micelles at both pH 5.0 and 7.4, with ζ -potentials of –5.2 and –8.1 mV, respectively.

Cytotoxicity of Micellar Systems. To understand the surface-charge-dependent cytotoxicity of the polymeric micelles, we tested four micelles against RAW 264.7 mouse macrophages. The surface chemistries of nanoparticles play a dominant role in determining their fate both in vitro and in vivo.^{45,46} Although it is easier to control the surface charge of inorganic nanoparticles,^{47–49} there is a limited understanding of the correlation between the cytotoxicity and the surface properties of polymeric micelles, due to the difficulty of preparing polymeric micelles with different surface charges and functionalities, while similar particle sizes are maintained. The micellar systems developed in this study had the same polymer backbone and similar sizes and size distribution characteristics (Figure 3), with various side chain functionalities that resulted

in micellar nanoparticles with various surface charges, which allowed for direct comparison of their biological properties.

Four micelles, 9–12, were tested for their cytotoxicity in RAW 264.7 mouse macrophages at different concentrations (Figure 5). No cytotoxicity was observed for the nonionic,

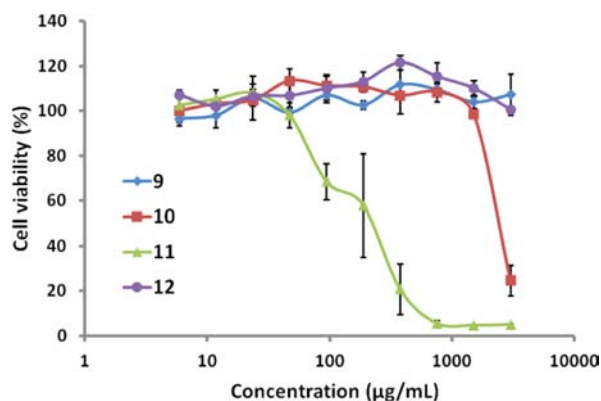


Figure 5. Cytotoxicity of the nonionic micelle 9, anionic micelle 10, cationic micelle 11, and zwitterionic micelle 12 in RAW 264.7 mouse macrophages after treatment at a concentration range of 5–3000 µg/mL for 24 h.

zwitterionic, and anionic micelles at the range of the tested concentrations (5–3000 µg/mL after 24 h incubation), except for the highest tested concentration of the anionic micelles. On the contrary, the cationic micelles showed a dose-dependent toxicity, which is in accordance with the known cytotoxicity of cationic nanoparticles, due to the interactions with the negatively charged cell membranes. As the cationic micelles may have potential applications as transfection reagents and nucleic acid delivery carriers, their cytotoxicity was compared with that of Lipofectamine, a commercially available cationic transfection agent. The IC_{50} value of the cationic micelles was 180 ± 48 µg/mL, while that of Lipofectamine was 31 ± 6 µg/mL. The approximately 6-fold lower cytotoxicity for the polyphosphoester-based cationic nanoparticles may result from the degradability or the surface characteristics of the system and may provide an alternative cationic carrier with better biocompatibility.⁵⁰ Due to their low toxicity, investigations of the transfection properties and their use in other biological applications are currently underway.

CONCLUSIONS

In this study, a retrosynthetic methodology has been used to develop a versatile platform for the construction of a family of polymeric micelles with varying surface charges and functionalities based on biodegradable polyphosphoesters. In this strategy, all steps of the entire engineering process, from small molecule chemistry to nanoparticle assembly, were equipped with click-type advantageous features, such as quantitative conversion, rapid reaction, mild conditions, high functional group tolerance, with an absence of byproducts and side reactions. The construction of the polymeric micelle system began from the preparation of hydrophobic and alkyne-functionalized monomers, continued through their polymerization, followed by chemical modification, and finally involved supramolecular assembly by direct addition of water. To overcome the hydrophilic nature of the polyphosphoester backbone, a hydrophobic monomer (2-ethylbutyl phospholane) was synthesized and its polymerization activity under two

organocatalysts was evaluated through the comparison with that of an alkyne-functionalized monomer butynyl phospholane. By taking advantage of the reactivity difference of the two monomers, the well-defined AB diblock polyphosphoester containing a hydrophobic block and a functional block was synthesized by an ultrafast ring-opening polymerization in a one-pot sequential manner. The clickable alkynyl groups on the functional portion of the hydrophobic-functional AB diblock polyphosphoester were transformed with four different thiols by photoinitiated, radical-mediated thiol–yne chemistry, forming four amphiphilic diblock polyphosphoesters with different charge types. Those nonionic, anionic, cationic, and zwitterionic amphiphilic diblock polyphosphoesters underwent self-assembly in water by direct dissolution and sonication to afford uniform spherical micelles with average sizes of ca. 15, 18, 18, and 23 nm (by TEM), respectively. The surface charges of those four micelles were found to coincide with the presence of their respective chemical functional groups. The micelles have also shown high biocompatibility, and even the cationic micelles had a 6-fold lower cytotoxicity when compared to Lipofectamine, a commercial transfection agent. Currently, this degradable nanoparticle family is being applied to various bioapplications.

ASSOCIATED CONTENT

Supporting Information

Detailed experimental section, synthetic scheme, and GPC data of failed diblock copolymer synthesis route and conditions, respectively. This material is available free of charge via the Internet at <http://pubs.acs.org>.

AUTHOR INFORMATION

Corresponding Author

wooley@chem.tamu.edu

Notes

The authors declare no competing financial interest.

ACKNOWLEDGMENTS

We gratefully acknowledge financial support from the National Heart Lung and Blood Institute of the National Institutes of Health as a Program of Excellence in Nanotechnology (HHSN268201000046C) and the National Science Foundation under grant numbers DMR-0906815 and DMR-1105304. The Welch Foundation is gratefully acknowledged for support through the W. T. Doherty-Welch Chair in Chemistry, Grant No. A-0001. The transmission electron microscopy facilities at Washington University in St. Louis, Department of Otolaryngology, Research Center for Auditory and Visual Studies funded by NIH P30 DC004665 are gratefully acknowledged. The authors thank Adriana Pavia for her kind assistance with illustrations.

REFERENCES

- Riehemann, K.; Schneider, S. W.; Luger, T. A.; Godin, B.; Ferrari, M.; Fuchs, H. *Angew. Chem., Int. Ed.* **2009**, *48*, 872.
- Yan, Y.; Such, G. K.; Johnston, A. P. R.; Best, J. P.; Caruso, F. *ACS Nano* **2012**, *6*, 3663.
- Singh, R.; Lillard, J. W. *Exp. Mol. Pathol.* **2009**, *86*, 215.
- Torchilin, V. P. *Adv. Drug. Delivery Rev.* **2006**, *58*, 1532.
- Ma, X.; Zhao, Y.; Liang, X. *Acc. Chem. Res.* **2011**, *44*, 1114.
- Elsababy, M.; Wooley, K. L. *J. Polym. Sci., Part A: Polym. Chem.* **2012**, *50*, 1869.

- (7) Kiesewetter, M. K.; Shin, E. J.; Hedrick, J. L.; Waymouth, R. M. *Macromolecules* **2010**, *43*, 2093.
- (8) Hawker, C. J.; Wooley, K. L. *Science* **2005**, *309*, 1200.
- (9) Iha, R. K.; Wooley, K. L.; Nystrom, A. M.; Burke, D. J.; Kade, M. J.; Hawker, C. J. *Chem. Rev.* **2009**, *109*, 5620.
- (10) Choi, H. S.; Ashitate, Y.; Lee, J. H.; Kim, S. H.; Matsui, A.; Insin, N.; Bawendi, M. G.; Semmler-Behnke, M.; Frangioni, J. V.; Tsuda, A. *Nat. Biotechnol.* **2010**, *28*, 1300.
- (11) Lee, S. M.; Chen, H.; O'Halloran, T. V.; Nguyen, S. T. *J. Am. Chem. Soc.* **2009**, *131*, 9311.
- (12) Zhang, S.; Li, Z.; Samarajeewa, S.; Sun, G.; Yang, C.; Wooley, K. L. *J. Am. Chem. Soc.* **2011**, *133*, 11046.
- (13) Ladmiraal, V.; Mantovani, G.; Clarkson, G. J.; Cauet, S.; Irwin, J. L.; Haddleton, D. M. *J. Am. Chem. Soc.* **2006**, *128*, 4823.
- (14) Liu, J.; Huang, W.; Pang, Y.; Huang, P.; Zhu, X.; Zhou, Y.; Yan, D. *Angew. Chem., Int. Ed.* **2011**, *50*, 9162.
- (15) Xiong, M.; Bao, Y.; Yang, X.; Wang, Y.; Sun, B.; Wang, J. *J. Am. Chem. Soc.* **2012**, *134*, 4355.
- (16) Wang, Y.; Yuan, Y.; Du, J.; Yang, X.; Wang, J. *Macromol. Biosci.* **2009**, *9*, 1154.
- (17) Zhang, S.; Li, A.; Zou, J.; Lin, L. Y.; Wooley, K. L. *ACS Macro Lett.* **2012**, *1*, 328.
- (18) Libiszowski, J.; Kaluzynski, K.; Penczek, S. *J. Polym. Sci., Part A: Polym. Chem.* **1978**, *16*, 1275.
- (19) Richards, M.; Dahiyat, B. I.; Arm, D. M.; Lin, S.; Leong, K. W. *J. Polym. Sci., Part A: Polym. Chem.* **1991**, *29*, 1157.
- (20) Pretula, J.; Kaluzynski, K.; Szymanski, R.; Penczek, S. *J. Polym. Sci., Part A: Polym. Chem.* **1999**, *37*, 1365.
- (21) Wen, J.; Zhuo, R. X. *Macromol. Rapid Commun.* **1998**, *19*, 641.
- (22) Liu, J.; Pang, Y.; Huang, W.; Zhai, X.; Zhu, X.; Zhou, Y.; Yan, D. *Macromolecules* **2010**, *43*, 8416.
- (23) Xiao, C.; Wang, Y.; Du, J.; Chen, X.; Wang, J. *Macromolecules* **2006**, *39*, 6825.
- (24) Iwasaki, Y.; Yamaguchi, E. *Macromolecules* **2010**, *43*, 2664.
- (25) Zhai, X.; Huang, W.; Liu, J.; Pang, Y.; Zhu, X.; Zhou, Y.; Yan, D. *Macromol. Biosci.* **2011**, *11*, 1603.
- (26) Yuan, Y.; Du, J.; Wang, J. *Chem. Commun.* **2012**, *48*, 570.
- (27) Clément, B.; Grignard, B.; Koole, L.; Jérôme, C.; Lecomte, P. *Macromolecules* **2012**, *45*, 4476.
- (28) Du, J.; Du, X.; Mao, C.; Wang, J. *J. Am. Chem. Soc.* **2011**, *133*, 17560.
- (29) Wang, Y.; Li, Y.; Yang, X.; Yuan, Y.; Yan, L.; Wang, J. *Macromolecules* **2009**, *42*, 3026.
- (30) Iwasaki, Y.; Wachiralapphaithoon, C.; Akiyoshi, K. *Macromolecules* **2007**, *40*, 8136.
- (31) Iwasaki, Y.; Nakagawa, C.; Ohtomi, M.; Ishihara, K.; Akiyoshi, K. *Biomacromolecules* **2004**, *5*, 1110.
- (32) Du, J.; Chen, D.; Wang, Y.; Xiao, C.; Lu, Y.; Wang, J.; Zhang, G. *Biomacromolecules* **2006**, *7*, 1898.
- (33) Zhu, W.; Sun, S.; Xu, N.; Gou, P.; Shen, Z. *J. Appl. Polym. Sci.* **2012**, *123*, 365.
- (34) Liu, J.; Huang, W.; Pang, Y.; Zhu, X.; Zhou, Y.; Yan, D. *Biomaterials* **2010**, *31*, 5643.
- (35) Liu, J. Y.; Pang, Y.; Huang, W.; Zhu, Z.; Zhu, X.; Zhou, Y.; Yan, D. *Biomacromolecules* **2011**, *12*, 2407.
- (36) Song, W.; Du, J.; Liu, N.; Dou, S.; Cheng, J.; Wang, J. *Macromolecules* **2008**, *41*, 6935.
- (37) Sun, T.; Du, J.; Yan, L.; Mao, H.; Wang, J. *Biomaterials* **2008**, *29*, 4348.
- (38) Sun, T.; Du, J.; Yao, Y.; Mao, C.; Dou, S.; Huang, S.; Zhang, P.; Leong, K. W.; Song, E. W.; Wang, J. *ACS Nano* **2011**, *5*, 1483.
- (39) Wang, Y.; Li, Y.; Sun, T.; Xiong, M.; Wu, J.; Yang, Y.; Wang, J. *Macromol. Rapid Commun.* **2010**, *31*, 1201.
- (40) Shao, H.; Zhang, M.; He, J.; Ni, P. *Polymer* **2012**, *53*, 2854.
- (41) Wachiralapphaithoon, C.; Iwasaki, Y.; Akiyoshi, K. *Biomaterials* **2007**, *28*, 984.
- (42) Wang, Y.; Tang, L.; Li, Y.; Wang, J. *Biomacromolecules* **2009**, *10*, 66.
- (43) Ober, C. K.; Cheng, S. Z. D.; Hammond, P. T.; Muthukumar, M.; Reichmanis, E.; Wooley, K. L.; Lodge, T. P. *Macromolecules* **2009**, *42*, 465.
- (44) Hoyle, C. E.; Lowe, A. B.; Bowman, C. N. *Chem. Soc. Rev.* **2010**, *39*, 1355.
- (45) Elsbahy, M.; Wooley, K. L. *Chem. Soc. Rev.* **2012**, *41*, 2545.
- (46) Albanese, A.; Tang, P. S.; Chan, W. C. W. *Annu. Rev. Biomed. Eng.* **2012**, *14*, 1.
- (47) Goodman, C. M.; McCusker, C. D.; Yilmaz, T.; Rotello, V. M. *Bioconjugate Chem.* **2004**, *15*, 897.
- (48) Arvizo, R. R.; Miranda, O. R.; Thompson, M. A.; Pabelick, C. M.; Bhattacharya, R.; Robertson, J. D.; Rotello, V. M.; Prakash, Y. S.; Mukherjee, P. *Nano Lett.* **2010**, *10*, 2543.
- (49) Walkey, C. D.; Olsen, J. B.; Guo, H. B.; Emili, A.; Chan, W. C. W. *J. Am. Chem. Soc.* **2012**, *134*, 2139.
- (50) Wang, J.; Mao, H.; Leong, K. W. *J. Am. Chem. Soc.* **2001**, *123*, 9480.